High Speed/Hypersonic Aircraft Propulsion Technology Development

Charles R. McClinton
Retired NASA LaRC
3724 Dewberry Lane
Saint James City, FL 33956
USA

Chuck.mcclinton@comcast.net

ABSTRACT

H. Julian Allen made an important observation in the 1958 21st Wright Brothers Lecture [1]: "Progress in aeronautics has been brought about more by revolutionary than evolutionary changes in methods of propulsion." Numerous studies performed over the past 50 years show potential benefits of higher speed flight systems – for aircraft, missiles and spacecraft. These vehicles will venture past classical supersonic speed, into hypersonic speed, where perfect gas laws no longer apply. The revolutionary method of propulsion which makes this possible is the Supersonic Combustion RAMJET, or SCRAMJET engine. Will revolutionary applications of air-breathing propulsion in the 21st century make space travel routine and intercontinental travel as easy as intercity travel is today? This presentation will reveal how this high speed propulsion system works, what type of aerospace systems will benefit, highlight challenges to development, discuss historic development (in the US as an example), highlight accomplishments of the X-43 scramjet-powered aircraft, and present what needs to be done next to complete this technology development.

1.0 HIGH SPEED AIRBREATHING ENGINES

1.1 Scramjet Engines

The scramjet uses a slightly modified Brayton Cycle [2] to produce power, similar to that used for both the classical ramjet and turbine engines. Air is compressed; fuel injected, mixed and burned to increase the air – or more accurately, the combustion products - temperature and pressure; then these combustion products are expanded. For the turbojet engine, air is mechanically compressed by work extracted from the combustor exhaust using a turbine. In principle, the ramjet and scramjet works the same. The forward motion of the vehicle compresses the air. Fuel is then injected into the compressed air and burned. Finally, the high-pressure combustion products expand through the nozzle and over the vehicle after body, elevating the surface pressure and effectively pushing the vehicle. Thrust is the result of increased kinetic energy between the initial and final states of the working fluid, or the summation of forces on the engine and vehicle surfaces. This is a modified Brayton cycle because the final state in the scramjet nozzle is generally not ambient.

Engine specific impulse, or the efficiency of airbreathing ramjet, scramjet and turbine engines, compared to the rocket is illustrated Figure 1. Specific impulse is the thrust (Nts) produced per unit mass flow (Kg/s) of propellant utilized, i.e. propellant which is carried on board. For the rocket, propellant includes fuel and oxidizer; for the air breather, fuel is the only propellant carried. Note the significant improvement in efficiency of the air breather vis-à-vis a rocket. For example, the scramjet is about 7 times more efficient than the rocket at Mach 7.

McClinton, C.R. (2008) High Speed/Hypersonic Aircraft Propulsion Technology Development. In *Advances on Propulsion Technology for High-Speed Aircraft* (pp. 1-1 – 1-32). Educational Notes RTO-EN-AVT-150, Paper 1. Neuilly-sur-Seine, France: RTO. Available from: http://www.rto.nato.int.

The revolutionary aspect of the scramjet is extending the airbreathing engine way beyond traditional aircraft limits. Subsonic combustion in the ramjet produces high static pressure and temperature and high heat transfer (heat load) to the engine combustor structure – especially at higher flight Mach number. These static temperature and heat loads place a practical upper limit on ramjet operation somewhere between Mach 6 and 8. The scramjet overcomes this limit using supersonic combustion. The scramjet has no nozzle throat at the end of the combustor. Supersonic combustion occurs at significantly reduced static pressure and temperature and hence combustor wall heat load. Reduced static temperature allows the practical upper limit of the scramjet to be somewhere between Mach 13 and 15. At the lower limit, the scramjet can be operated below Mach 6 using mixed-mode combustion. At these speeds fuel is injected near the exit of the expanding combustor. Combustion pressure rise disturbs and separates the inflowing boundary layer. This disturbance propagates upstream through the boundary layer, creating a large recirculation region. The supersonic inlet flow is farther compressed by this separated/recirculating flow to Mach 1, which then persists through the initial combustion region, before again accelerating supersonically through the remaining combustor and nozzle. Combustion in this process occurs both in the recirculating flow and in the sonic/supersonic core – hence the term mixed mode combustion. The fact that a scramjet can be designed to operate in both pure supersonic or mixed combustion modes, covering both the ramjet and scramjet operating speeds, led to the label dual-mode scramjet.

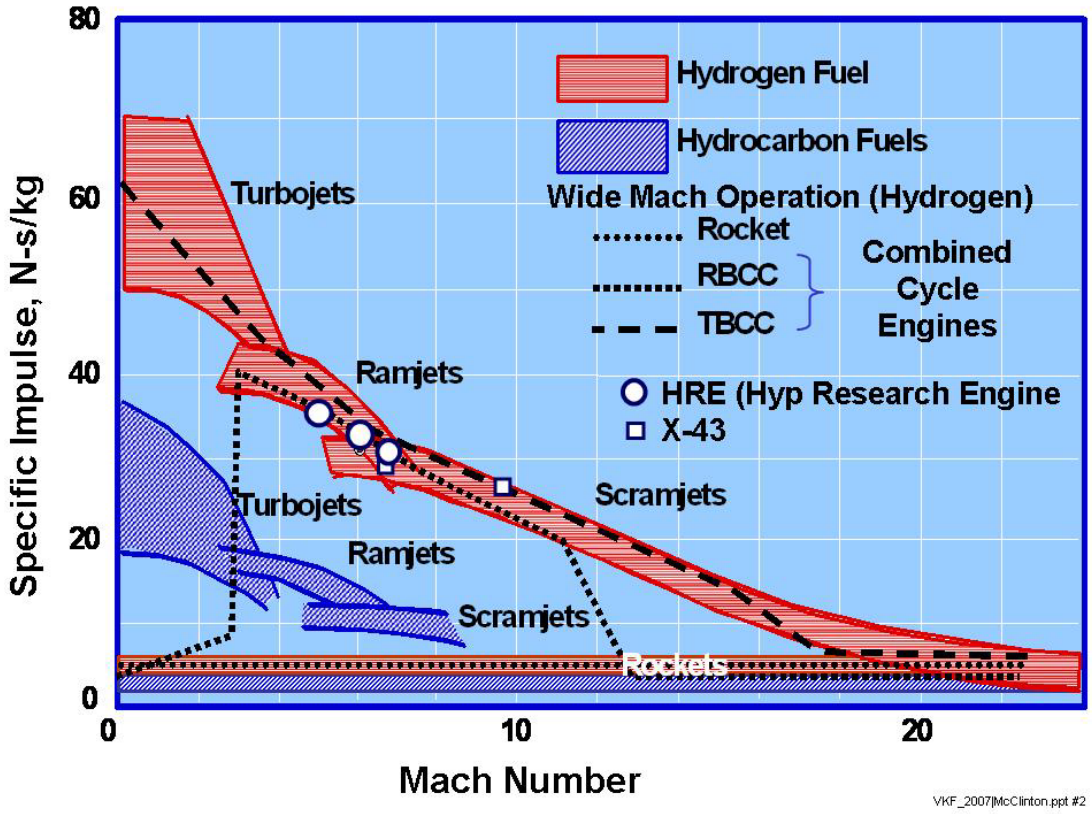

Figure 1. Hypersonic Engine Efficiency

1.2 Combination/Combined Cycle Engines

The dual-mode scramjet can operate over the ramjet and scramjet speed range, from about Mach 3 to at least Mach 15. Any application of the scramjet will require an alternate means of accelerating to scramjet takeover speeds. For an aircraft application alternate power will be required to allow efficient operation below Mach 3-4 for take off, acceleration, and deceleration to powered landing. A study [3] performed by Marquardt, Rocketdyne and Lockheed, in the early 1960's, provided a low-level (of fidelity) assessment of numerous propulsion options for space access. In all, 36 potential rocket/airbreathing systems were compared. These combined cycle engines included rocket, air-augmented rocket, ramjet, and scramjet cycles. In addition, various "air compression" concepts for low-speed operation were considered, including ejector, fan, and the liquid air cycle (LACE). These studies evaluated as a figure of merit vehicle capability (payload to space for a 1-million pound vehicle). Two conclusions from this study are: Scramjet operation to high Mach provides a significant increase in payload capability; Lox usage below scramjet takeover Mach number greatly lowers the payload capability. Three engines were recommended for additional study: Turbine-scramjet combination engine; ScramLACE; and Supercharged Ejector Ramjet (SERJ). The ScramLACE is an ejector-scramjet with real-time liquid-air collection and compression feeding a hydrogen-air rocket ejector. The SERJ is an ejector ramjet with fan for operation during acceleration to Mach 2 and cruise. The three systems were studied in the USA, and only the turbine-scramjet approach was carried forward. For airbreathing launch vehicles, an additional propulsion system is required for higher-speed operation to achieve orbital velocity, and rockets are the only option. Because the rocket is required for high speed and orbital insertion for single-stage-to-orbit (SSTO) concepts, several studies have also reconsidered it for low-speed operation (albeit inconsistent with the previous [3] conclusions). The resulting engine is called a rocket-based combined cycle engine. Dashed lines in figure 1 illustrate the potential efficiency of the turbine-scramjet-rocket combination (TBCC) engine and the RBCC engines studied extensively in the late 1990's by NASA.

The RBCC design challenges include rocket placement, rocket fuel-oxidized mixture ratio, and the impact of rocket integration on scramjet performance. One RBCC concept is illustrated in figure 2. This concept [4] operates in air-augmented rocket (AAR) mode from Mach 0 to about 3. This mode includes some ejector benefit by entraining air into the dual-mode scramjet duct. Above Mach 3 the rocket is turned off, and the engine operates as a dual-mode scramjet. The final mode of operation, rocket, begins at Mach 10. In rocket mode the engine inlet is eventually closed before the vehicle leaves the atmosphere.

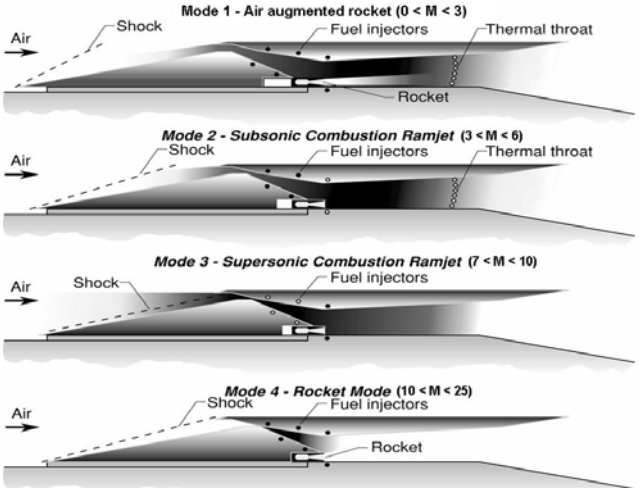

Figure 2. - RBCC Operating Modes

NASA and the USAF have studied turbine-based "over-under" combination engine (TBCC) approaches at a low level for over 40 years. Most of the studies use "simple" over-under designs [5], as illustrated in figure 3**.** These designs all utilized variable geometry inlet and nozzles which can fully close to seal off either engine.

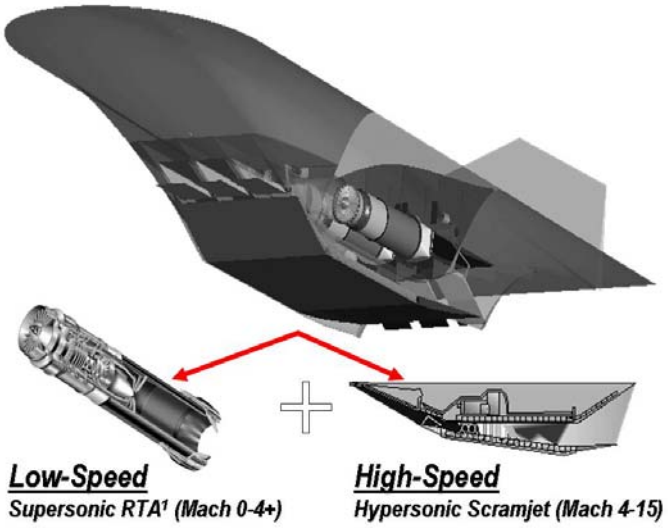

Figure 3. - Typical TBCC

2.0 AIRCRAFT APPLICATIONS

Numerous studies performed over past 50 years show potential benefits of higher speed flight systems – aircraft, missiles and space craft. Potential airbreathing high speed/hypersonic vehicle applications include endoatmospheric and space access. These vehicles may be military or civilian, manned or unmanned, reusable or expendable, hydrocarbon or hydrogen fueled. Potential applications include tactical supersonic cruise—hypersonic dash, hypersonic cruise strategic aircraft, hypersonic tactical or strategic missile, hypersonic transports, and fully or partially reusable single or two-stage-to-orbit (TSTO) launch systems.

2.1 Military Applications

Military benefits of hypersonic vehicles are versatility, response time, survivability, and unfueled range [6]. Civilian benefits are long range rapid commercial transportation and safe, affordable reliable and flexible transportation to low-earth orbit [7]. One example of a potential hypersonic cruise military aircraft is the Dual-Fuel Global-Reach concept shown in Figure 4. It would employ hydrocarbon-fueled turbo-ramjet engines for low-speed flight (Mach 0 to 4.5) and liquid hydrogen-fueled scramjet engines for high-speed flight (Mach 4.5 to 10). This vehicle concept was developed to perform two candidate operational scenarios. The baseline mission involves takeoff, climb to cruising altitude and Mach number, complete a cruise to a mission range of 15,000 Km, followed by a 2.5 g turn at the target at minimum power, and unpowered, maximum L/D descent for rendezvous with a tanker, and a subsonic return to base. The vehicle contains sufficient hydrogen to reach and engage the target, turn, and begin the unpowered descent. Sufficient hydrocarbon fuel is retained on board to allow a 10 minute loiter waiting for the tanker. An alternate mission scenario is a first stage platform for satellite launch. The resulting vehicle is comparable in size and weight to today's air liners, as illustrated in figure 4.

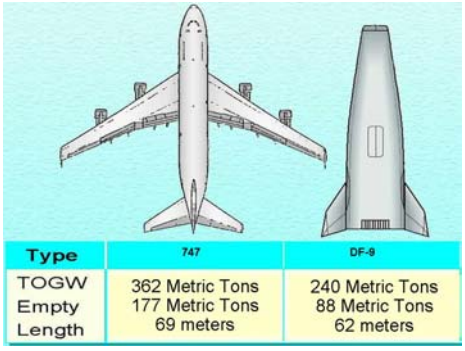

Figure 4. –Strategic Hypersonic Aircraft

2.2 Space Launch Applications

Benefits [7] of air-breathing launch systems are improved safety, mission flexibility, vehicle design robustness and reduced operating costs. Air-breathing vehicles, capable of hypersonic speeds, can transform access to space, just like turbojets transformed the airline business. Rocket-powered vehicles are approaching their limits in terms of these parameters [7]; switching to a new approach is the only way to achieve significant improvements [5].

Safety benefits result from characteristics such as enhanced abort capability and moderate power density. Horizontal takeoff and powered landing allows the ability to abort over most of the flight, both ascent and decent. High lift/drag (L/D) allows longer-range glide for large landing footprint. Power density, or the quantity of propellant pumped for a given thrust level, is 1/10 that of a vertical take off rocket due to lower thrust loading (T/W), lower vehicle weight and higher specific impulse. Power density is a large factor in catastrophic failures. Recent analysis [8] indicates that safety increases by several orders of magnitude are possible using air-breathing systems. Mission flexibility results from horizontal takeoff and landing, the large landing (unpowered) footprint and high L/D. Utilization of aerodynamic forces rather than thrust allows efficient orbital plane changes during ascent, and expanded launch window. Robustness and reliability can be built into airbreathing systems because of large margins and reduced weight growth sensitivity, and the low thrust required for smaller, horizontal takeoff systems. Cost models [7] indicate about one-order magnitude reduction in operating cost is possible, vis-à-vis the space shuttle. Attributes for selected air-breathing assisted launch systems categorized by staging Mach number and reusable or expendable second stage are listed in Table 1.

Table 1. Attribute of Space Launch Systems

Attributes	Baseline ELV	Baseline Space Shuttle	Mach 7 Stage	Mach 10 Stage	Mach 15 Stage	SSTO
	Expend-able	Partially Reusable	Expendable 2nd Stage	Reusable	Reusable	Reusable
Payload Fraction	3%	1%	1-2%	3%	4%	5%
Loss of Vehicle/Pay load	1: 50	1: 100	1: 4,000	1: 60,000	1: 110,000	1: 160,000
Cost per Lb to LEO	$2,500	$10,000	$1,700	$2,000	$1,400	$1,000

NASA's Next Generation Launch Technology Program identified and quantified these attributes [7, 8]. For example, staging at Mach 7, and using an expendable second stage allows nearly an order of magnitude gain in safety (loss of vehicle/payload), with a small improvement in payload fraction and operating cost, compared with current systems (Space Shuttle or ELV's). Increasing staging Mach number (the fraction of airbreathing contribution to orbital velocity) plus adding a reusable second stage and more advanced engine and airframe technology, increases the payload fraction and reliability, and reduces both loss of vehicle (LOV) and operating cost. The most significant benefit is in safety, quantified by the attribute "Loss of Vehicle."

Airbreathing hypersonic flight is truly the next frontier for air vehicle design, and continues to excite and challenge the next generation of engineers and scientists. What will be the first application?? That depends on political forces more than on technology development challenges. In terms of difficulty, easiest first: hypersonic cruise missile; supersonic cruise - hypersonic dash tactical aircraft; Mach 7 first stage launch vehicle; Mach 7 hypersonic cruise strategic aircraft; Mach 10-15 first stage launch vehicle; Mach 10 cruise; and finally single-stage to orbit launch vehicle.

3.0 CHALLENGES

Challenges facing development and applications of scramjet engines to hypersonic airbreathing propulsion systems are technical and political. Political challenges are beyond the scope of this discussion – but must be seriously addressed in any effort to apply this technology. Technical challenges can be divided into the following categories: Flow physics; Experimental facilities and test methods; Design methods; Scramjet propulsion-airframe integration; High/low-speed engine integration; Flight testing; and Technology development tracking.

3.1 Airframe Integrated Scramjet Design Challenges

The most significant challenges facing design and development of a hypersonic vehicle are propulsion related: scramjet engine design; scramjet-airframe integration; integration of the scramjet with a Mach 4 capable low-speed engine. Effective utilization of scramjets requires careful integration of the airframe and engine. This is required because of the large airflow requirements at high speed. As flight speed increases, the air flow enthalpy approaches, then at about Mach 8 exceeds, the incremental enthalpy increase from combustion, so thrust per unit air flow decreases. This effect is captured by Aaron Auslender's "rule of 69": $T \sim m_{air} * SQRT (69 / M^2)$ for Mach numbers greater than 7.

With a high degree of propulsion-airframe integration, vehicle flight operations affect the engine operation, mostly through changes in air mass capture. Conversely, engine operation affects vehicle performance, such as lift and trim. Challenges in design/development of airframe integrated scramjets are illustrated using the 2-D cross section of the X-43 scramjet-powered research vehicle in figure 5. The X-43 was a sharp-leading edge lifting body configuration. That is, vehicle lift is generated by the vehicle fuselage and engine, not wings. The vehicle wings were really all moving elevon surfaces for maintaining and controlling vehicle pitch and roll attitude. The entire lower surface of the X-43 was designed to perform scramjet functions, within the limit of acceptable hypersonic aerodynamics, stability and control. The top surface was designed to minimize form drag, enclosing the vehicle between the inlet leading edge (vehicle nose), and the nozzle trailing edge (vehicle tail). Generally good scramjet cycle performance requires that the nozzle is about 30% larger than the inlet capture cross-sectional area. Much of the scramjet inlet compression and nozzle expansion is performed on the vehicle forebody and after body respectively, so that the engine module can remain as short as possible. Short internal engine length is desirable because it is the densest structure on the vehicle, and large surface areas will drive up weight and cooling requirements, potentially exceeding fuel flow requirements. The engine cowl, or lower

surface is positioned to capture all of the flow compressed (behind the bow shock wave) on the lower surface at the most critical flight condition, or design point. For hypersonic cruise the design point is the fully loaded cruise condition; for an accelerator it is somewhere close to the peak airbreathing Mach number.

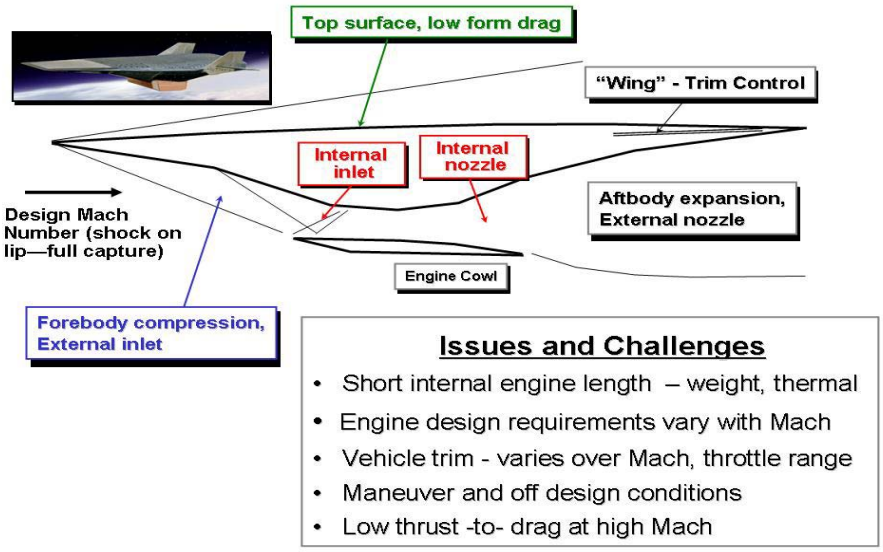

Figure 5. Airframe Integrated Scramjet Design Challenges

Airframe integration and scramjet engine design is challenged because the vehicle must operate over a large Mach number range, and be capable of maneuvering. Airframe integration includes the effect of the vehicle on the engine performance, as well as engine on the vehicle. At lower than design Mach number the shock waves and hence the compressed flow moves away from the vehicle, so some compressed air is not captured. As the vehicle maneuvers, the shocks move closer on the lifting side, again changing the air capture. Conversely, the engine performance affects the vehicle design and operation. One significant integration issue is the vehicle pitching moment change with flight Mach number. Generally the higher mass capture at high Mach number allows the engine to produced higher pressure on the external nozzle than that on the forebody produced by aerodynamic compression, so the vehicle tends to pitch down. At lower Mach number, much of the air compressed by the forebody is not captured by the engine. Fortunately, the combustor pressure rise is greater at lower Mach number, but generally not sufficient to make up for spilled air mass flow. So, at low Mach the vehicle tends to have a nose-up pitching moment, which is balanced by the control surfaces. Clearly, as the thrust requirement from the engine changes, the nozzle pressure will change the vehicle pitching moment and trim requirement, because the inlet forces are essentially constant.

In addition to these challenges, even the engine flowpath design requirements vary with Mach number. For example, the inlet compression, expressed by contraction ratio, must be smaller at low Mach number, and increase nearly 1:1 with flight Mach at constant flight dynamic pressure. This is required to allow the inlet to start and function at lower speeds, and provide adequate static pressure in the combustor for good combustion at higher speeds. The shape of the combustor and/or fuel injection location must vary with Mach number to assure good combustor operation. Combustion must start close to the combustor entrance for very high Mach operation, and the combustor must be short. For low speed, the fuel must be injected at a point in the combustor where sufficient expansion has already occurred to minimize the potential for un-starting the inlet. At low speed, an

inlet isolator is critical for good performance, at high speed it is a serious detriment to performance. These challenges are addressed by variable geometry, multiple fuel injection stations, or both.

Many different shapes of scramjets were studied in the USA and around the world. Many have focused on the quasi two-dimensional shape selected for the X-43 engine. Others utilized swept sidewall compression [10], conical axisymmetric [11], inward turning axisymetric [12] (with and without a centerbody), and fully three-dimensional [13]. These concepts all share the same challenges in regards to high speed/hypersonic physics – and they all have about the same performance at the design point. The discriminator between competing configurations has generally been off design performance, operability and weight. Performance issues are often associated with combustor flow distortion. For operation over a significant flight envelope (more than a range of a few Mach numbers), variable geometry is inevitable. Generally this is limited to inlet contraction and throttling the air flow to the inlet, for inlet starting, thrust control and inlet close-off. This variable geometry is accomplished by linear movement of body panels, engine cowl, center body plugs, or fuel injectors.

Hypersonic propulsion physics challenges include: Natural and forced boundary layer transition; Boundary layer turbulence; Separation caused by shock-boundary layer interaction; Shock-shock interaction heating; Inlet isolator shock trains; Cold-wall heat transfer; Fuel injection, penetration and mixing; Finite rate chemical kinetics; Turbulence-chemistry interaction; Boundary layer relaminarization; Recombination chemistry; and Catalytic wall effects. Each of these phenomena must be understood and either modeled or avoided, to successfully develop a scramjet engine. Models for these phenomena are usually developed from test data gathered in “unit” experiments which isolated and focus on the phenomena.

Integration of the high speed scramjet with the low speed engine – such as a turbo-ramjet – requires blending/sharing structure, systems and flowpaths where ever possible. Interestingly, many studies have shown the major design consideration is thrust per unit volume, not per unit engine weight for TBCC engines. Another challenge is flight acceptance testing of these propulsion systems.

3.2 Design methods

Systems studies are required to identify potential vehicle configurations, and focused technology development. For an airbreathing vehicle, systems studies are complicated by the highly integrated and coupled nature of the airframe and engine [14]. Integration aspects previously discussed confirm the need to develop the engine in concert with a specific class of vision or reference vehicle. “Coupled” means that performance of each successive component is dependent on performance of the previous components. For example, the nozzle component efficiency can not be independently determined; it is dependent on flight Mach number and vehicle attitude, as well as inlet, isolator, and combustor design, operability and performance. Therefore, the vehicle and engine are designed together, using sophisticated analysis methods. A typical design process is illustrated in Figure 6. This process requires a vehicle characterized to the point that meaningful analysis can be performed. Engine and aerodynamic performance, structure, weight, systems and packaging, and thermal management are iterated as the vehicle is “flown” to determine the volume of propellant “required”. Finally, the vehicle is resized to package the propellant required to meet the mission, thus defining a "closed" configuration.

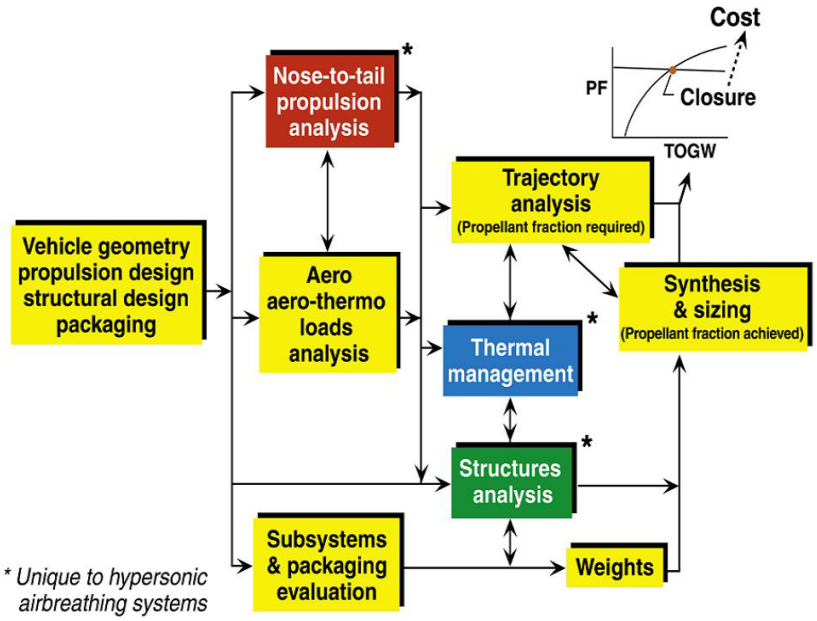

Figure 6. – Hypersonic Vehicle Design System

Systems analysis methods for airbreathing vehicles have evolved dramatically, yet a wide range in usage remains. These methods can be executed at several levels [14], as noted in Table 2. This discussion will focus only on propulsion tools. The lowest level scramjet design tool is ideal or approximate cycle analysis. The next level is cycle analysis using plug in efficiencies which are externally estimated or determined for a particular configuration as a function of flight Mach number only. The next level is CFD – which has its own sublevels. If the CFD analysis is validated by comparison with representative unit and engine component test data, it represents a step up in fidelity. The highest fidelity is obtained by engine tests in a wind tunnel, or preferably in flight. The wind tunnel tests are a lower fidelity than flight because the results must be scaled by analysis to flight conditions. Uncertainty in predicted performance and operability decreases with higher level analysis methods. At the lowest 0^{th} level performance could easily be off by 50-100% or more, and the engine not operable. At the highest level, performance within 1-2% is anticipated. This table is presented as a guide to help assess the large disparity in analytical results and projected vehicle capabilities. A good design process requires synergistic utilization of experimental, analytical and computational analysis. Configurations discussed in section 2 were developed using level 2 methods, and uncertainty on the order of 10% is expected. In fact, the payload fraction for the Mach 15 first stage vehicle in Table 1 is approximately 50% of the payload fraction estimated in the original 0^{th} level 1965 study [3] discussed in section 1.2.

Table 2. – Design Methods and Vehicle Level of Fidelity Assessment.

Level	Color Code	Propulsion	Aero	Structure Weight	Vehicle Performance	Synthesis & Packaging
3	Blue	Flight Data	Flight Data	Flight Vehicle	Flight Vehicle Performance	Flight Vehicle
	Light Blue	Wind Tunnel Data	Wind Tunnel Data	Components Fab/Test	6-DOF Hardware Simulation	Mock-up, CAD Multi-Eqn. Non-linear
2	Green	CFD Certified	CFD Certified	FEM Certified	3-DOF/ 6 DOF Trimmed	CAD Multi-Eqn. Non-linear
	Light Green	Cycle Certified	Engineering Methods Certified	Unit Loads Certified	3-DOF Trimmed	CAD Multi-Eqn Non-Linear
1	Yellow	CFD Uncertified	CFD Uncertified	FEM Uncertified	3-DOF untrimmed	Single Eqn., Non-linear
	Orange	Cycle Uncertified	Engineering Methods Uncertified	Unit Loads Uncertified	Energy State	Single Eqn. Linear
0	Red	Ideal Cycle	L/D, Cd Estimated	Design Tables	Rocket Equation	Estimated

3.3 Design Optimization

Due to the relatively small excess thrust generated by a scramjet, some method is needed to refine designs to improved performance and to define operability limits. Scramjets are particularly benefited by a formal optimization process because of significant propulsion-airframe interdependence, large number of independent variables, large potential range of variables, significant interactions, non-linearity and the current low level of design optimization. In addition, it has been clearly demonstrated that component optimization does not provide the best engine or vehicle. Figure of merit (FOM) in this optimization can be engine thrust, but vehicle level FOMs are better, such as minimum vehicle size/weight for mission, cost, safety, or other system level factors.

Several optimization approaches were considered for hypersonic systems. Design-of-experiments (DOE) [15, 16] was selected by the USA hypersonic community because it can be used with existing analysis and experimental methods. By using DOE, a large number of independent variables can be investigated efficiently. DOE uses statistical methods to build polynomial approximate models for the response (component or system performance) to multiple independent design variables. Because of the analytical nature of these models, multiple regression analysis can be used to evaluate these models. The performance model can either be optimized or quantified to determine most significant design variables.

Design-of-experiments (DOE) studies within the Hyper-X community utilized the central composite design (CCD) approach [16] to define an experimental test or analysis matrix. The CCD technique is a part of response surface methodology [17] by which the relationship between the response (dependent variable) and a set of independent variables can be established. Responses are generated for all points in the test or analysis matrix. For Hyper-X, this was accomplished either by CFD, analytical, experimental, or complete system analysis. Response surfaces are then generated for the individual responses.

For a complicated system such as a scramjet or hypersonic vehicle, non-linearity and strong two-parameter interactions are expected. Thus, at least three levels for each of the design parameters are required in order to

capture nonlinear effects. Therefore, a second-order model as shown in eqn. (1) is essential: x_i terms are the independent design parameters that affect the response variable y, and the b terms are regression coefficients.

$$y = b_0 + \underbrace{\sum_{i=1}^{n} b_i x_i}_{\text{linear}} + \underbrace{\sum_{i=1}^{n} b_{ii} x_i}_{\text{non-linear}} + \underbrace{\sum_{i=1}^{n} \sum_{\substack{j=1 \\ j \neq i}}^{n} b_{ij} x_i x_j^2}_{\text{two-parameter interaction}} \qquad (1)$$

The number of analyses or experiments for the CCD method compared to those for a full factorial design is illustrated in Table 2 of reference [18]. Many studies focus on 8 variables, which represent 6587 points in a full factorial design, but only require 81 points in a CCD.

An example application for design of flush wall fuel injectors [18], included the following independent variables: θ, Injection angle (90 degrees is normal to the wall); $P_{t,j}$, Injector total pressure; ϕ, Fuel equivalence ratio; FS, Fuel splits (film fraction of total injectant); HS, Injector spacing to gap ratio (h/Gap – where Gap is the smallest dimension of the combustor cross section at injector plane); M, Flight Mach number; and Xc, Combustor length (Normalized by Gap). The CCD matrix was solved using 3-D CFD in the combustor and nozzle, and 2-D for the forebody and inlet. Responses extracted from the solutions and modelled included mixing and combustion efficiency, total pressure recovery and entropy, combustor wall heat transfer (peak and total), combustor shear drag, one-dimensional variation of pressure, temperature, Mach number and flow distortion [9] through the combustor, nozzle thrust coefficient, and combustor thrust potential [2]. An example of the response models - the fuel mixing efficiency is:

η_{mix} = 0.0364+0.5668*(FS)+0.249*(HS)+0.2223*(Φ)+0.0002026*(θ)-0.2973*M+0.000011925*$P_{T,J}$
+0.0002031*(θ)*M-0.3492*(FS)*(Φ -0.2133*(FS)*(HS)-0.003980*(FS)*(θ)-0.0857*(HS)*(Φ)+1.696*Xc
-0.1103*(Xc^3)-0.00588*(FS)*Xc^2-0.3104*(FS)*Xc-0.4134*(HS)*EXP(-24*EXP(-2*Xc))
+0.0376*(Φ)*EXP(-20*EXP(-2*Xc))+0.063*M*((Xc-2)^2) -0.00035*(θ)*Xc^2+0.00004*$P_{T,J}$*(Xc-0.5)^0.6 (2)

This study was performed without a complete vehicle design team, so it used combustor thrust potential to define the optimum flush wall injector design. Thrust potential is the best estimate of engine thrust resulting from changes in fuel injector design. Figure 7 illustrates the best engine thrust potential from this study at Mach 10 with ϕ = 1.0. Characteristics of the "best" fuel injector are presented in figure 7. Note that thrust potential peaks at a combustor length of 18 gaps, then decreases if the combustor is extended. This is a result of slow fuel mixing/combustion adding less energy than that removed by friction, heat transfer and nozzle energy lost to combustor dissociation. The corresponding fuel mixing efficiency for this "optimum thrust" design is about 80% at a combustor length of 18 gaps. A combustor length of about 35 Gaps is required to achieve 95% mixing with this injector, and the thrust loss incurred by extending the combustor is large. This example illustrates the necessity of designing each component to benefit the system, not just the component efficiency itself. Comparison with high quality non-reacting data has shown that the CFD prediction of fuel mixing for this study is accurate to within 5% [19]. (This is an example of design tools, not a recommended design solution).

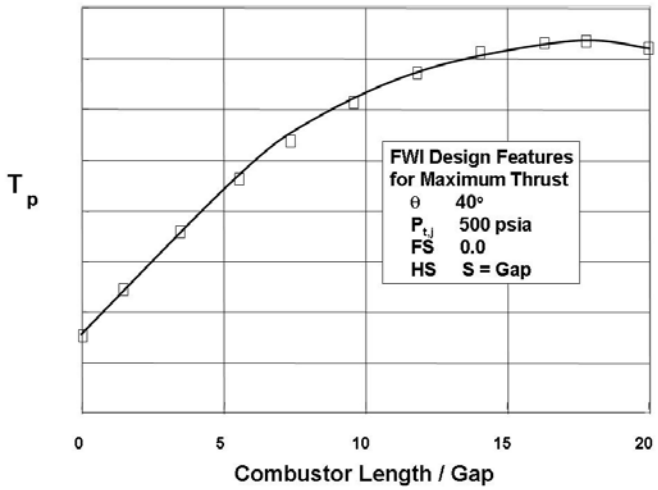

Figure 7. Typical Result from DOE Study: Combustor Thrust Potential

3.4 Experimental facilities, measurements and test methodology

Scramjet engine and hypersonic vehicle development requires an integral design and systems engineering approach. Experimental testing is utilized for developing an understanding of physics, developing models, and validating design concepts and design tools. The enthalpy and pressure requirements for hypersonic combustion simulation are summarized in [9]. The sensible total enthalpy of flight increases from 6 to 12 MJ/kg as flight Mach increases from Mach 10 to 15. The forebody flow field and inlet compression process reduce the local Mach number and raise the flow static pressure along a nearly constant total enthalpy path. The combustor entrance Mach number, stagnation temperature, and stagnation pressure for Mach 10 flight simulation are 3, 3800 K, and 100 atm, and for Mach 15 are 5, 7000 K and 2000 atm. respectively. As pointed out above, combustion heat release produces about the same energy increment as the air kinetic energy at Mach 8. Thus, simulation of supersonic combustion flow conditions for propulsion studies in ground test facilities often utilizes so-called direct-combustion heating with oxygen replenishment as a means of generating the test environment. Other sources of energy such as storage heaters, electric arc heaters, or shock compression can also provide the required energy and pressure levels for some tests. Combustion heated facilities and combustion heated storage facilities are capable of generating enthalpy and pressure requirements for simulation to about Mach 8. Arc heated facilities are capable of extremely high enthalpy, but are limited to 50 atmospheres pressure, about Mach 8 requirements. Shock heated wind tunnels are required for higher flight Mach simulation. Reflected shock tunnels, with stagnated test gas expanded in converging-diverging nozzle, are capable of a few millisecond test time, at up to about Mach 10 flight simulation; expansion tunnels are capable of flight simulation to over Mach 15 with less than one millisecond test duration.

Four types of scramjet testing are generally performed: Unit problems – to understand the hypersonic flow field physics; Component tests – to verify inlet, isolator, combustor or nozzle component performance and operability before testing the complete engine; Integrated flowpath (inlet, combustor nozzle including or not including vehicle effects); And engine tests – to verify the thermal management heat exchanger durability, engine structure, and systems.

Some unit experiment simulations require full enthalpy. Boundary layer transition, shock impingement heating, and fuel mixing simulation requirements do not necessitate full enthalpy. However, combustion and

recombination finite rate chemistry unit studies require full enthalpy. Component testing of inlets, isolators and nozzles to some extent, allow partial simulation of enthalpy at full Mach and Reynolds number. Simulation of the combustor, or the nozzle recombination chemistry, or component integration requires full flight enthalpy. Four methods of scramjet engine and/or flowpath testing are typically utilized: direct-connect, semi direct connect, semi free jet, and free jet tests.

Direct-connect tests are utilized for combustor or combustor nozzle integration studies and combustor nozzle thermal/structural validation. The scramjet combustor (or inlet isolator) is connected directly to the test gas heater by a supersonic facility nozzle, to provide the correct Mach, total pressure and enthalpy of the air flow. This approach allows the highest flight Mach number simulation for any pressure-limited heater, by bypassing inlet losses. Semi-direct-connect experiments are similar – although the combustor does not capture all of the heated airflow. This approach is useful to bypass hardware development. These two approaches are useful for combustor development, but do not provide the inflow required to refine the combustor design, or assess inlet interaction (issue only at lower Mach, M<8). Integrated flow path or engine testing is generally performed using the semi-free-jet approach. The engine module (internal flowpath) is fully replicated, but the external inlet and nozzle parts of the vehicle are only partially or not at all included, allowing a larger scale test. This approach has been used extensively in the USA, and is discussed in numerous papers [20-22]. Free-jet testing includes the entire length of the engine flowpath, generally from the vehicle nose to tail. This type of test can only be performed at small scale or for small engines. The NASA Hypersonic Research Engine, the Central Institute of Aviation Motors (CIAM) scramjet [23] and the X-43 full vehicle were all tested in this fashion.

Measurements in high enthalpy and pressure supersonic or hypersonic flow are difficult. Therefore measurements are generally limited to pre combustion flow surveys, forces and moment, wall pressure and temperature, and non-intrusive optical approaches. Much of the information of interest must be deduced from measurements which are sensitive to competing unknowns. Wall pressure, the easiest measurement, is dependent on combustion, shear, heat transfer, fuel injection, mixing and shock entropy losses. Some of these effects can be measured, others modeled, but the net effect is increased uncertainty on combustion efficiency deduced from wall pressure measurements. Never the less, this deduced combustion efficiency has proven adequate at lower Mach numbers, in continuous flow facilities. At higher speeds this deduced combustion efficiency becomes large, as the impact of combustion on pressure rise becomes smaller. An in-depth study of measurement requirements was performed by Bittner [24, 9]. This study showed that for flight Mach 10-15 scramjet designs, fuel mixing and combustion efficiency are the most important combustor performance parameters (i.e., engine thrust is about proportional to combustion efficiency). Considering the measurement uncertainty and sensitivity of indirect measurements for deducing mixing and combustion efficiency, Bittner concluded that these performance parameters must be directly measured. The best experimental measurement for determining combustion efficiency is combustor exit water mass fraction (determined by line-of-sight laser absorption), and for mixing efficiency, is fuel mass fraction distribution. Bittner demonstrated, by evaluation of typical CFD solutions, that 3 or 4 - 0.50 mm diameter laser absorption paths for a combustor with 3 cm gap are adequate to resolve the combustion efficiency at any cross section to +/- 5 percent uncertainty. To isolate finite rate chemistry from fuel mixing completeness, a measure of fuel mixing is also important. Bittner's recommendation was to use the process Rogers [25] defined as fuel plume imaging, by tracing the injected fluid with very small (0.2 microns in diameter) particles. Illumination of a cross plane in the flow with laser light can then produce a Mie scattering image of the particles which can be recorded with a fast electronic camera and thus visualize the fuel distribution in the experiment. The local amount of reflected light in each image, normalized by the average reflected light in each plane, becomes a measure of the local fuel concentration relative to the average concentration in the overall bulk flow. Thus, this technique allows a quantitative measure of the fuel distribution to be determined with successive pictures at successive planes downstream from the injection location in the duct. This method has been shown consistent with CFD to less than ± 10% uncertainty.

3.5 Flight Testing

Flight testing remains an important element in hypersonic propulsion and vehicle development. Flight not only provides the real environment, it also requires a different look at priorities. In wind tunnels, fuel equivalence ratio is important and thrust produced is secondary – in flight thrust is the priority, and how you get it is secondary. In the wind tunnel testing, engine pitching moment and lift are interesting concepts, and occasionally measured. In flight pitching moment is critical to vehicle survival. In the wind tunnel, inlet starting is an exercise about the ideal design condition – in flight it is a multidimensional challenge involving not only the current flight condition, but the flight history. Flight is expensive, and the benefits are not fully known. Flight testing immature concepts is expensive, high risk, and gives flight testing a bad reputation. But flight testing previously developed and wind-tunnel tested concepts is essential to completing the technology development.

3.6 Technology Development Tracking

Significant advancements in hypersonic technology were made over the past 50 years. These technologies address hypersonic airframe, engine and systems development. The state of technology, expressed by Technology Readiness Level (TRL), was documented by the National Aerospace Plane Program [26] (NASP), NASA Langley Research Center [27] (LaRC), NASA Space Launch Initiative's Next Generation Launch Vehicle Technology program [28], the 2004 National Research Council (NRC) review [29] of The National Aerospace Initiative (NAI) Hypersonics Pillar, and Boeing [30]. A typical vehicle-based work breakdown structure (WBS) used to guide TRL tracking [28] of hypersonic launch vehicle technology development progress is presented in Appendix A of reference [31]. A work breakdown structure (WBS) is required to define the system elements or needed products to assure that the reported TRL is relevant. Tracking technology development is important to help focus development. It is also important for the end user to assure technology is truly ready for application to his needs. NASA research was established to elevate the TRL to "6", i.e. test of integrated system in a relevant environment – at which point it may be considered for system development [32].

Technology status for the Mach 7 first stage of a two stage-to-orbit launch system and estimates to complete the technology will be discussed in the final section of this paper.

4.0 HISTORICAL PERSPECTIVE

Early history of scramjet development is documented by Curran [33] and Anderson [9]. A well known Air Force view of what followed the early feasibility studies is of cyclic "fits and starts" [34]. This resulted from over zealous efforts to simultaneously develop and apply hypersonic technology to programs which were on a classical 5-year development cycle. NASA perspective is of an incremental development process, which benefited from the "fits and starts" to fund major advancements.

NASA has, for nearly 50 years, funded hypersonic airbreathing vehicle technology development, aiming at futuristic space launch capabilities. NASA's activities can be divided into five generations of technology development. The first was associated with the DOD Dyna Soar/Aerospace Plane and NASA's focus on developing hypersonic vehicle technology. This phase included hypersonic airframe and engine, aerothermodynamics, structures and propulsion performance. The propulsion focus was proof of scramjet cycle efficiency, flight weight engine structure, and engine system integration. Starting in the mid 60's, NASA built and tested a hydrogen fueled and cooled scramjet engine [11] which verified scramjet cycle efficiency, structural integrity, first generation design tools and engine system integration. The axisymmetric engine selected allowed a low risk approach to validate the scramjet cycle and elementary design tools of the day.

NASA's second generation hypersonic technology starting in the early 1970's focused on scramjet-airframe integration [10]. NASA designed and demonstrated, in wind tunnels, a fixed-geometry airframe-integrated scramjet "flowpath" and companion vehicle capable of accelerating to Mach 7. In the process, wind tunnels, test techniques, leading-edge cooling, and analytical methods were all advanced, and 3-D CFD was first applied to the scramjet reacting flow.

Starting in the early 80's, NASA teamed with the DOD in the National AeroSpace Plane (NASP) Program to advance and demonstrate hypersonic technologies required for a scramjet based combined cycle powered, single-stage to orbit (SSTO) launch vehicle. Under the NASP program NASA focused on technology development and risk reduction, including: system analysis, aerodynamics, flight controls, high temperature structures, aerothermodynamics, hypersonic physics, scramjet engine detailed analysis and testing, hydrogen cooled engine structure, and hypersonic flight testing.

Following NASP, NASA's fourth generation hypersonic technology development focused on flight validation of hypersonic technology and evaluation of alternate concepts (rather than SSTO) for the next generation of space access. Flight tests included a scramjet [23] designed and flown by the Central Institute of Aviation Motors (CIAM), a low-speed takeoff and landing version of the X-43 [35], and finally the X-43 at Mach 7 and 10. Highlights of the X-43 flight program are presented in the next section. All of these tests demonstrated the need for flight testing to re-focus technology development. They also prove that flight testing does not have to be expensive. Evaluation of alternate, near term space access configurations was instrumental in developing advanced system analysis methods, particularly assessment of system level benefits, and system engineering tracking of technology development status and requirements.

Fifth generation hypersonic technology development within NASA started in 2005. President Bush's unfunded redirection of NASA to manned space exploration resulted in significant programmatic changes within NASA aeronautics and sciences. NASA management was required to maintain NASA's unique hypersonic capability (manpower and some facilities), and did this by refocusing on low-cost in-house low-TRL research studies [32, 36], avoiding even low-cost high payoff higher TRL efforts such as developing a durable metallic scramjet combustor as mentioned in section 6.0. Fortunately, DOD is continuing hypersonic technology advancements within some of the National Aerospace Initiative (NAI) [6] programs, and some NASA's expertise is being applied to support these DOD programs, particularly the USAF X-51 missile research demonstrator [37].

5.0 X-43 FLIGHT HIGHLIGHTS

5.1 Hyper-X Program Development

NASA developed the concept for the Hyper-X Program and X-43 vehicle in 1995/96 in response to several "blue-ribbon" panel recommendations that flight demonstration of airframe-integrated scramjet propulsion be the next step in hypersonic research. The experts agreed that at a minimum and as a first step a vehicle must fly with scramjet power to validate airframe-integrated scramjet performance and design methods. A two-phase flight and ground based research program was approved by the NASA administrator in 1996: focus of the first phase was the X-43; focus of the second phase was to be development and flight test of the "low speed" turbojet engine integrated with the scramjet forming a complete hypersonic propulsion system. This section discusses accomplishments of the Phase 1 program. The next section presents results from the planning for the Phase 2 program.

The NASA Hyper-X Program employed a low cost approach to design, build, and flight test three small, airframe integrated scramjet-powered research vehicles at Mach 7 and 10. The Hyper-X team developed the X-

43 phase 1 vehicle [38] as a small-scale, hydrogen-fueled research vehicle to provide flight data for an airframe-integrated scramjet engine flowpath. (The engines were heat sink cooled to meet program budget and schedule. Regenerative cooling was not needed due to the short test times afforded with a small vehicle.) In addition, data were obtained for aerodynamic, thermal, structure, guidance, flush-air-data-system and integrated system analysis design method validation. Test plans called for boosting each of three X-43 research vehicles to the required test condition by a drop-away booster. The research vehicles were dropped from the NASA B-52, rocket-boosted to test point by a modified Pegasus first stage, separated from the booster, and then operated in autonomous flight. Tests were conducted at approximately 30 kilometre altitude at a nominal dynamic pressure of 0.47 atm (1000 psf). The resulting vehicle was 3.7 km long and weighed about 1270 kg. Development of the X-43 and its systems are well documented [23, 38-49]. The first Mach 7 flight was attempted June 2, 2001. This flight failed when the Pegasus booster went out of control early in the flight. The second and third flights were successfully conducted March 27 and November 16, 2004. This section provides an overview of results (with engine focus) from the second and third flight of the X-43. Details of the launch vehicle development, verification, validation and integration, flight operations [50-54] and other results are well documented.

5.2 Flight Test Trajectory

For the second (Mach 7) flight (F2) the launch vehicle was dropped from the B-52 flying at Mach 0.8 and 12.2 km altitude. The booster ignited after a 5-second free fall. The launch vehicle executed a 1.9g pull-up, followed by a 0.7g pushover to achieve nearly level flight at 30 km. altitude. Following burnout, stage separation, and X-43 vehicle stabilization, the engine cowl was opened for about 30 seconds: 5 seconds of fuel-off tare, 10 seconds of powered flight (at about Mach 6.83 and dynamic pressure of 463 atm), another 5-seconds of un-powered steady tare, followed by 10 seconds of Parameter IDentification (PID) maneuvers [55]. The PID maneuver was designed to quantify the aerodynamic stability and control parameters for the vehicle, including drag, to allow more accurate estimation of the engine thrust. After the open-cowl PID maneuver, the engine cowl closed, and the vehicle flew a controlled descent over 560 km to “splash-down” in the Pacific Ocean. PID maneuvers were flown at various Mach numbers as the vehicle slowed and descended.

The third flight (F3) trajectory was somewhat different. The B-52 flight conditions were the same. However, the launch vehicle executed a 2.5g pull-up to a flight path angle of over 30 degrees, followed by a 0.5g push over to achieve nearly level flight at 33.5 km altitude. Following burnout, stage separation, and stabilization of the X-43 vehicle, the engine cowl was opened for about 20 seconds: 3 seconds of fuel-off tare, 11 seconds of powered flight (at about Mach 9.68 and dynamic pressure of 0.439 atm.), and another 6-seconds of un-powered steady tare. (No cowl open parameter identification maneuvers were performed due to cowl survival concerns that necessitated closing the cowl immediately following the cowl open tare.) The engine cowl closed, and the vehicle flew a controlled descent over 1600 km to a “splash-down” in the Pacific Ocean. During the descent PID maneuvers were successfully performed [56] at successive Mach number as the vehicle slowed down.

5.3 Instrumentation, Measurements and Data

The X-43 vehicles were well instrumented. Instrumentation included over 200 measurements of surface pressure, over 100 thermocouples to measure surface, structural and environmental temperatures, and discrete local strain measurements on the hot wing and tail structures. The flight management unit included accurate 3-axis measurements of translational acceleration and angular velocity, along with Global Positioning System and control surface deflection measurements. Instrumentation density is illustrated in figure 8 by external and internal wall pressure and temperature on the lower body surface. Internal engine instrumentation, within the cowl on the body side is denser to capture internal flow details (shock waves) within the engine.

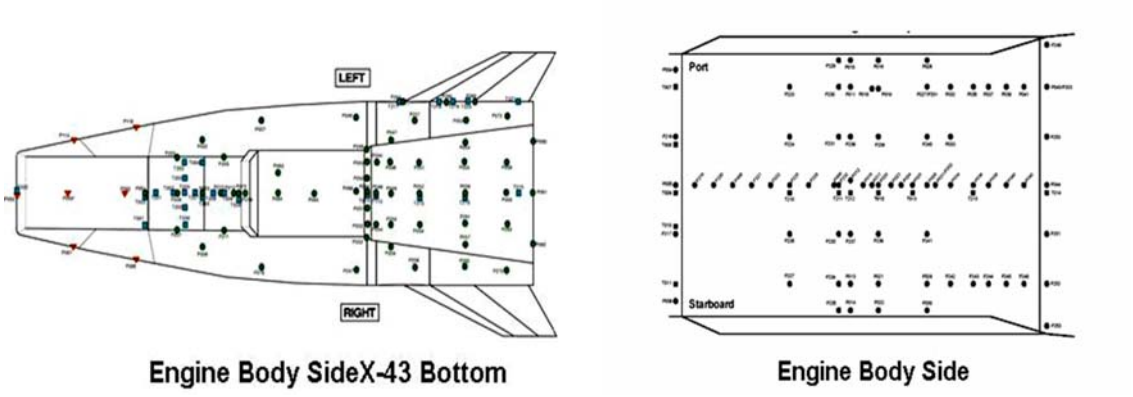

Figure 8. X-43 Instrumentation and Measurements (Circle – pressure; Square – Temperature)

All of the data from the X-43 flights were successfully telemetered and captured by multiple air and ground stations. The instrumentation health and performance were excellent: very few lost instruments/parameters; very low noise content; no significant calibration issues; no significant delay or time lag issues; and extremely limited telemetry stream drop outs. Accuracy of these measurements benefited from day-of-flight atmospheric measurements by weather balloons. These measurements were used in flight trajectory reconstruction [57], and resulted in a small change in calculated Mach number and dynamic pressure vis-à-vis real time values determined from atmospheric tables and winds from historical atmospheric tables. Flight 2 best estimated trajectories (BET) resulted in higher dynamic pressure and Mach, but only a trivial change in AOA. Flight 3 BET resulted in lower dynamic pressure and higher Mach and AOA. The flight test data from both flights F2 and F3 fully satisfied the Hyper-X Program objective to validate experimental, analytical and computational design methods, plus demonstration of positive acceleration under scramjet power.

5.4 Stage Separation

Following the rocket motor burnout, the launch vehicle targeted flight conditions for stage separation: 0° angle of attack (AOA-alpha) and yaw (Beta); zero pitch, yaw and roll rates; and dynamic pressure of 0.47 atm. The indicated Mach was slightly low for flight 2. Post test analysis indicates that off-nominal rocket motor propellant temperature was the major factor affecting burnout and hence the reduced Mach number at F2 stage separation. The research vehicle separation from the booster was executed cleanly [57]. The X-43 attitude was within less than 1-sigma uncertainty from the predicted nominal by pre-flight Monte Carlo analysis.

5.5 Scramjet Powered Flight Control

For flight 2, the X-43 was commanded to fly at 2.5° angle of attack during the cowl-open portion of the flight. However, as the fuel was turned-on/off, and throttle adjusted, the engine pitching moment changed significantly. Figure 9a illustrates the measured angle of attack—from cowl open to fuel off and the start of the Mach 7 PIDs. During the scramjet-powered segment, the AOA was maintained at 2.5° ± 0.2°, except during flameout, which occurred as the fuel was shut off. (The flight control system included some feed-forward control). For flight 3, the vehicle was commanded to fly 1.0° angle of attack during the cowl open segment. The vehicle control was about the same, as illustrated in figure 9b. For both F2 and F3 the fuel sequencing for powered flight started with a silane/hydrogen mixture to assure ignition, then transition to pure hydrogen fuel. The ignition sequence for F2 required about 1.5 seconds. With transition to pure hydrogen fuel, the engine control was designed to ramp the throttle up (increase fuel mass flow) to either a predetermined or controlled maximum value (limited by inlet

unstart monitor), and then decreased as the fuel was depleted. The resulting vehicle performance is characterized by vehicle acceleration, as shown in figure 9. The ignition sequence for F3 was different—the silane remained on for the first two fueled conditions, requiring 5 seconds of silane pilot. Then the same fuel equivalence ratio conditions were tested with only hydrogen. This cautious approach was taken because it was not possible to transition from piloted to unpiloted operation in the short test time available in shock tunnels, and some unpiloted wind tunnel data had poor combustion.

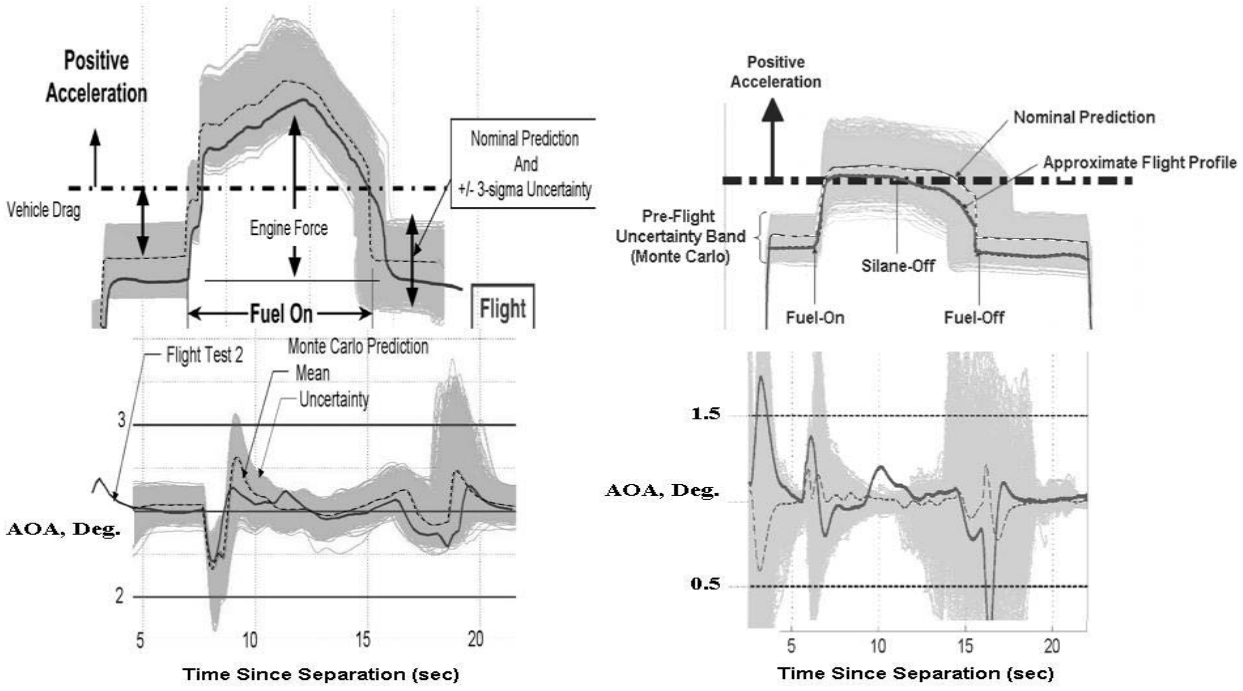

A) Flight 2 at Mach 7 **b) Flight 3 at Mach 9.7**

Figure 9. X-43 vehicle acceleration and angle of attack (AOA)

5.6 Scramjet Engine Performance

Gray bands in figure 9 illustrate pre-test Monte Carlo predictions of acceleration and angle of attack about the nominal prediction (dashed line). The heavy solid line depicts flight data trends. The vehicle deceleration is greater than predicted [58], both with cowl closed and open. This is because of two factors: actual flight conditions (2/3 of the difference); and vehicle drag was higher than predicted (1/3 of the difference). However, the drag was within the uncertainty associated with the aerodynamic database. The uncertainty was not resolved before flight because it did not threaten the outcome of the engine tests. Under scramjet power the F2 vehicle acceleration was positive, and varied with throttle position. The increment in acceleration is about as predicted, which confirms the predicted engine thrust to within less than 2% (ref. 5 and 6). It should be noted that the engine throttle was varied over a large range without incurring engine "un-start" or "blow-out." Under scramjet power the F3 vehicle cruised (thrust = drag) at the reference fuel equivalence ratio with 2% silane pilot, and the engine force was in agreement with predictions [58].

5.7 Validation of Scramjet Design Analysis

Predicted scramjet performance is also confirmed by the excellent comparison of pre-test predicted and flight scramjet flowpath wall pressure (fig. 10). Data are presented from vehicle nose to tail for F2 (fig. 10(a)), and from cowl leading edge to cowl trailing edge for F3 (fig. 10(b)). Mach 7 data showed the scramjet operating in "dual mode," with sonic flow in the isolator dissipating the inlet shocks at the design throttle position. Mach 10 data exhibits classical pure supersonic combustion mode, i.e. the combustor pressure is shock dominated. The pre-test prediction for Mach 7 was made using the coupled CFD-cycle code SRGULL [59-61], with combustion efficiency determined by analysis of multiple wind tunnel tests, most notably the 2.5 meter diameter test section of the *8-Foot High Temperature Tunnel* (HTT) test [46] of the Hyper-X Flight Engine (HXFE) on the Full Vehicle Simulator (FVS). The Mach 10 pretest prediction was performed using a combination of CFD tools, with the SHIP code [62] used for the combustor. The SHIP code is space marching with uncoupled reaction modelling – both to reduce solution times and allow very fine grid resolution for the complex shock structure. The reaction efficiency used in the SHIP code was derived from analysis of engine tests conducted in the HYPULSE and LENS reflected shock tunnels. Storch [59, 63] and Ferlemann [64] present a detailed discussion of these codes and the pretest predictions for F2 and F3 respectively.

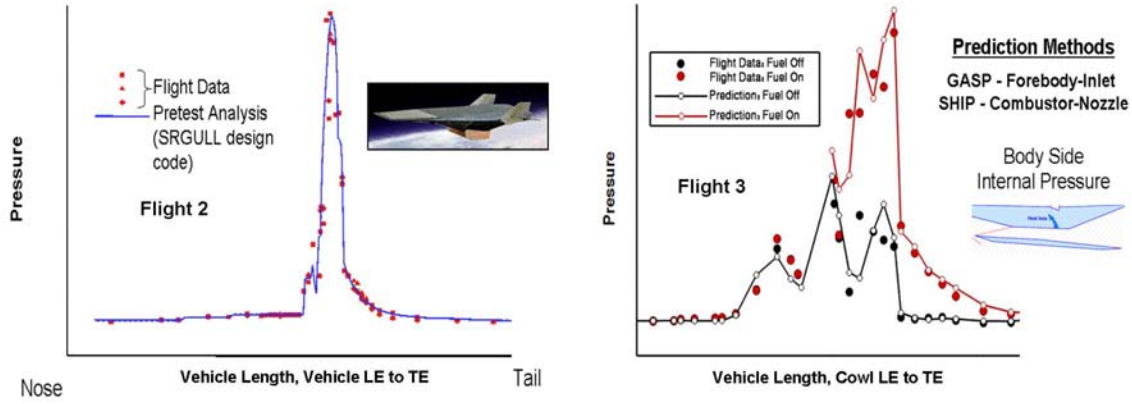

a) Flight 2 at Mach 7 **b) Flight 3 at Mach 9.7**

Figure 10. Comparison of engine body side wall pressure with pre-flight predictions

Post test analyses of the flight data model the "as flown" trajectory to assess thermal loads, inlet mass capture, boundary layer state for boundary layer transition assessment, and to assess the overall vehicle drag, engine force, and vehicle acceleration at exact flight conditions/control positions. Complete nose-to-tail CFD solutions for the actual F2 flight condition include solutions for closed cowl, cowl open, and powered operation, (fig. 11). These solutions show excellent agreement with flight acceleration data.

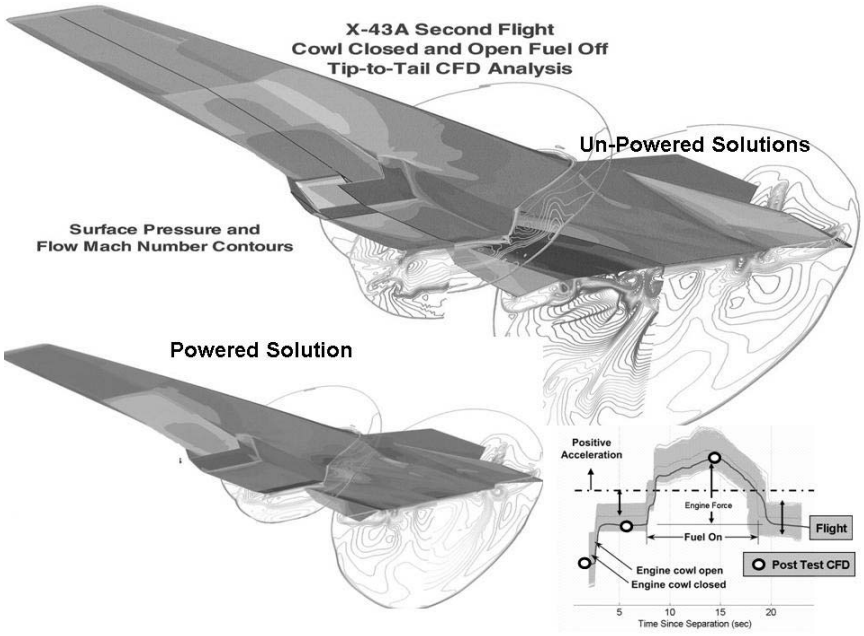

Figure 11. Post Test CFD Analysis

5.8 Validation of Scramjet Experimental Methods

Flight 2 (F2) data compare favorably with measurements made in four separate wind tunnel tests [63] and F3 flight data compare favourably with results from both the HyPulse and LENS shock tunnel tests [64]. Tests with nearly identical values of fuel equivalence ratio were selected for comparison. Wind tunnel wall pressure measurements were scaled by air mass capture ratio to flight conditions. Flight air mass capture is calculated by 3-D CFD analysis of the forebody. Figure 12 illustrates the resulting comparison of internal wall pressure for the 8-Foot High Temperature Tunnel test of the Hyper-X Flight Engine (HXFE) on the Full Flight Vehicle Simulator (FFS). Similar agreement was noted between flight data and data produced using semi-free jet engine module tests in shock heated, combustion heated and electric arc heated wind tunnels. Storch [59] discusses the implication of this agreement, and the impact on observed combustor performance.

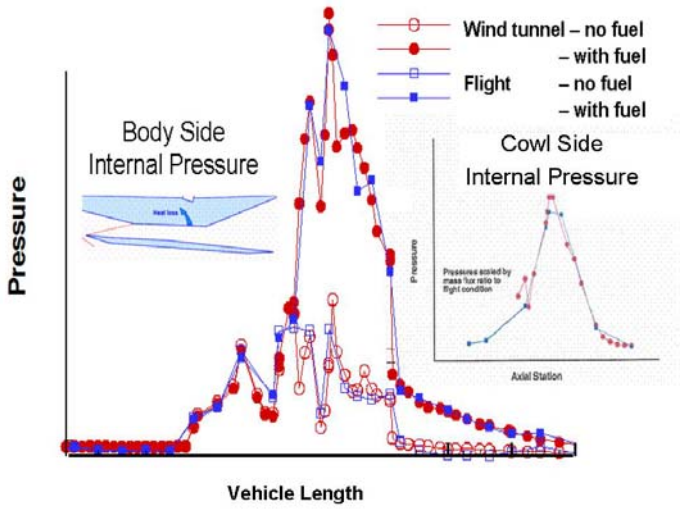

Figure 12. Comparison of flight and Wind Tunnel Data.

Rogers [65] reported a similar trend for the Mach 10, flight 3 data. Results show that ground tests are representative of flight when careful attention is paid to modeling the important flow phenomena. The most significant issues identified for shock tunnel testing are cold wall temperature limitation and attention to correct shock position entering the combustor for the shock-dominated "pure" scramjet operation. This means that the vehicle/engine geometry may have to be changed for tests in typically non-uniform shock tunnel flow fields to truly represent important flight features. This was successfully demonstrated by Rogers [65].

5.9 Hypersonic Boundary Layer Transition

Design of the X-43 research vehicle structure and thermal protection system depended greatly on accurate estimation of the aerothermal environment, which required understanding of the boundary layer state during the entire flight. For good engine operation, boundary layer flow entering the inlet cannot be laminar. For the X-43, boundary layer trips were required to insure the inlet boundary layer was turbulent to limit flow separations due to adverse pressure gradients. A substantial research and design effort [45] was executed to ensure proper sizing of boundary layer trips with minimum induced trip drag, excess vorticity and induced heating. The vehicle upper surface, however, was predicted to be laminar during the scramjet test, based on a pre-flight trajectory, using a classical transition methodology (momentum thickness Reynolds number over the boundary layer edge Mach number of $R_{e,\theta}/M_e$ = 305). Figure 13 provides upper surface temperature time histories during the first 350 seconds of flight 2 trajectory from the point of release from the B-52. The three upper surface thermocouples were evenly spaced along the vehicle centerline starting about midpoint for T/C#19 and ending near the trailing edge for T/C#21. Note that by the time the cowl opens and the scramjet is ignited, the entire upper surface appears to be laminar, as indicated by the dramatic temperature decrease that begins at about 70 sec. Likewise, at about 240 seconds the boundary layer transitions from laminar to turbulent as the vehicle slows. The pre-flight predictions, using the classical approach, were accurate (300±12) in estimating these latter transition points along the flight trajectory. However, the transition from turbulent to laminar earlier in the flight occurred at a local $R_{e,\theta}/ M_e$ = 400. Thus the laminar to turbulent and turbulent to laminar transition criteria are not the same, and the X-43 measurements provide flight data that quantify the hysteresis effect [66]. The first transition, from turbulent to laminar, represents the condition for which the transition model was developed - the high heating condition encountered as the hypersonic vehicle accelerates within the high dynamic pressure airbreathing

corridor. These results show that the classical boundary layer transition model was not appropriate for application to the boost trajectory. It is hoped that the new, more advanced "physics – based" methods for boundary layer transition can be applied correctly to this problem.

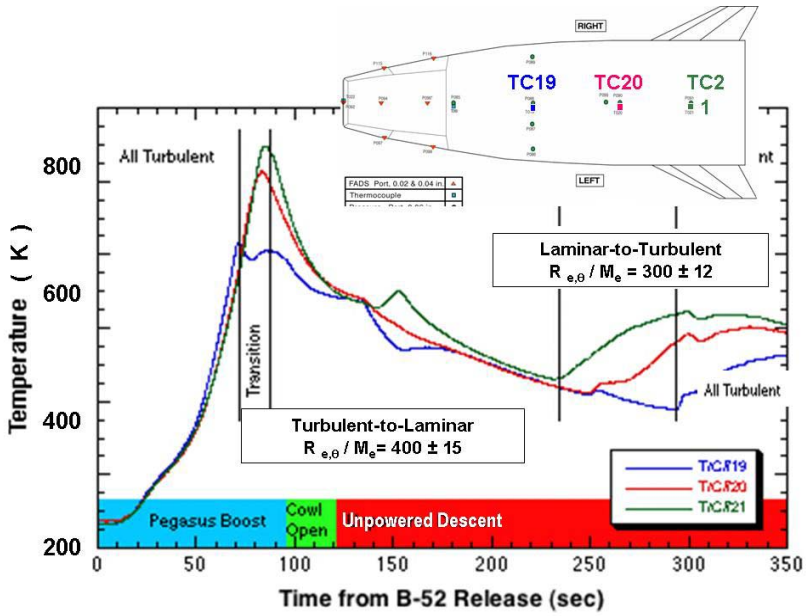

Figure 13 – Natural Boundary Layer Transition

Post test analysis determined the engine efficiency (specific impulse) achieved in the X-43 flights, and "scaled" that value to a vision vehicle performance, by removing effects of small physical (viscous dominated) scale, cold fuel, cold engine wall temperature, off-nominal fuel equivalence ratio, operating dynamic pressure, etc. The scaled specific impulse is within the capability band projected for scramjet engines, as indicated by the square symbols in figure 1. The specific and effective impulse demonstrated by the X-43 has set the bar for follow-on vehicle configurations.

5.10 Validation of Vehicle System Analysis

As discussed herein and in [67], most of the measurements and performance results from the two successful flight tests confirm the design methods, test methodologies, and capabilities of proposed hypersonic air vehicles. Most of the measured performance values were within predicted uncertainties. This included propulsion performance and operability, aerodynamic forces and moments, stability and control, aero thermal heating, structural responses, and the complex mechanics of high Mach, high dynamic pressure, non-symmetric stage separation. Included in this hypersonic environment are many physics challenges, discussed in section 3.1. Most of these phenomena were modeled in the design tools. Others were avoided by application of a large uncertainty. Success of the X-43 demonstrates an engineering level understanding of the hypersonic physics. A better understanding of the physics might be beneficial for reducing the uncertainty in optimization of vehicle performance—but the current understanding is clearly adequate to continue higher-level technology development and integration. Design and analysis tools demonstrated in the Hyper-X program are clearly adequate for hypersonic vehicle development.

5.11 Technology Achievements

Technology achievements [67] of the X-43 include the first ever test of a scramjet-powered vehicle in a wind tunnel and in flight. The flight also proved the performance, operability and control of an airframe integrated engine – vehicle system. In addition, these results provide information which will allow higher fidelity (i.e. reduced uncertainty) in future system studies. Data and performance from the flight test verified engineering application of the NASA – Industry – University hypersonic vehicle design tools. To support this development, NASA's HyPulse facility at GASL was modified to be the first facility capable of operation in both reflected and expansion tunnel mode, allowing scramjet testing from Mach 7 to Mach 15 plus in a single wind tunnel.

5.12 Lessons Learned

Lessons learned from the Hyper-X Program's X-43 flight are infinite and remain a permanent part of the experience base of each participant. From a management perspective several lessons should be noted. First, a lesson handed down over generations – build on the shoulders of Giants, not babies (the "not invented here" approach). This includes selecting the team to execute the program, as well as selecting the configuration and approach to minimize new technology development requirements. Second, plan the program to fit budget and schedule, with a healthy reserve of both. Next, fight requirements creep. Fourth, utilize a small team of 'hands-on' experts, and empower them, but maintain good communication (even co-location) with and between them. Finally, beware of outside experts and strap hangers, carefully consider recommendation before including them in program changes.

From a technology perspective the major lesson is that a scramjet powered vehicle performs as advertised. A close second was that going to flight required all disciplines to sharpen their pencils. For example, early NASA predictions for scramjet pitching moment were off by over 25%, and the first prediction of stagnation heating did not include real gas effects. Regarding scramjet technology, flight performance was better than obtained in reflected shock tunnels – probably due to the higher wall temperature in flight. Combustor isolator pressure rise was slightly greater in wind tunnel than in flight. The biggest surprise came from the most mature technology – boundary layer transition. Hysteresis effects had not been considered in the classical boundary layer transition modelling. So, in effect, the boundary layer transition models developed over the past 40 years for the server ascent flight of airbreathing hypersonic vehicles were shown to be only appropriate for re-entry vehicles, not the airbreathing hypersonic vehicle flight corridor. A similar lesson was learned from the CIAM/NASA scramjet flight test [68, 69]. Analysis at the design Mach 6 flight test condition (top and left side of figure 14) predicted excellent inlet flow despite rather strong internal shock waves. Flight data and post test analysis showed that the inlet starting process created a large separation bubble (right side of figure 14) at lower flight Mach number, and the separated flow remained at the design point.

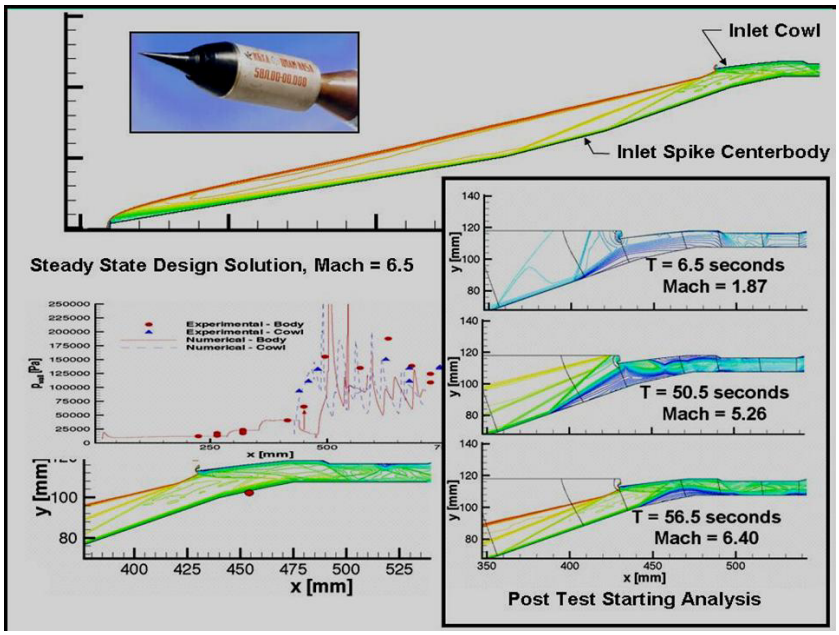

Figure 14. – CIAM Inlet Solutions: Pre and Post Test.

6.0 FUTURE NEEDS AND CHALLENGES

This section addresses the question: "After the successful flight test of the X-43 scramjet-powered vehicle, what is the TRL for a near term hypersonic vehicle, and what needs to be done next?"

Technology status for the Mach 7 first stage vehicle of a TSTO system is summarized in figure 15. Clearly the technology set for a Mach 7 vehicle is less challenging than for the SSTO or higher Mach air-breathing first stage of a two-stage-to-orbit concept. For example, all of the airframe technologies are at least TRL 5-6 and required propulsion performance is at least TRL 5-6. Programs to complete the technology to TRL 6 were recently estimated by a NASA planning activity for the Hyper-X Phase 2 Program. Details of the airbreathing propulsion technology shortfalls (TRL < 6) for the first stage Mach 0-7 vehicle are discussed in the following sub-sections. Other technology short falls not included herein - High Temperature Materials and Thermal Protection System (TPS); Propellant Tanks; Integrated Vehicle Design and MDO Tools; and Expander Cycle Linear Aero-spike Rocket - are discussed in reference [31, 67].

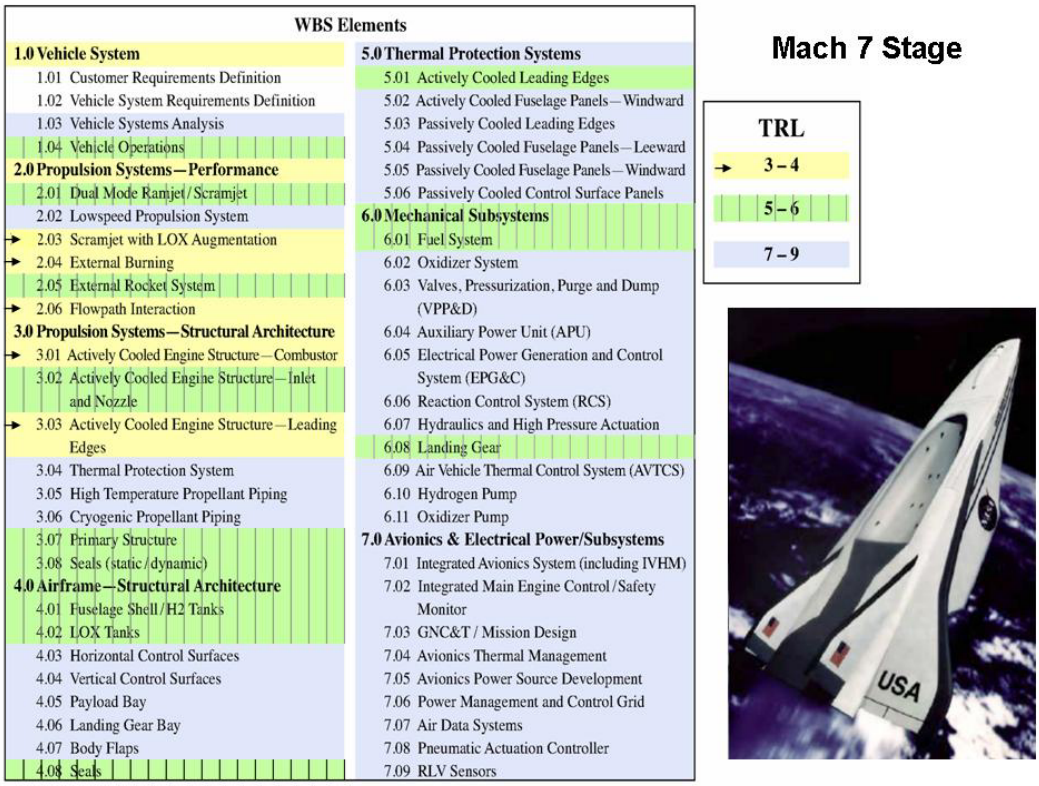

Figure 15. - Technology Status for First Stage of a TSTO Airbreathing Launch System

This propulsion discussion continues to assume that the first application space access vehicle will incorporate the turbine-based combination cycle engine system – i.e. a two-flowpath engine in either an "over-under" arrangement or separately integrated into the airframe. The low-speed engine is assumed to be the NASA/GE Revolutionary Turbine Accelerator (RTA) [70] or equivalent hydrocarbon-fueled turbo-ramjet engine, with uninstalled thrust-to-weight (T/W) of about 10. This engine must dash to Mach 4, with about 2-minute full power operation required above Mach 2.

The high-speed engine is a quasi two dimensional hydrogen-fueled and cooled dual-mode scramjet. Extensive databases exist for flowpath designs for good engine performance and operability, from Mach 4 to 7. Key technical challenges for the dual-mode scramjet are low Mach number (M<4) performance and operability (TRL 4-5); demonstration of durable fixed or variable geometry metallic structure and seals (TRL 5); development and demonstration of robust engine controls for large operating range; optimization of aero-propulsion integration, and development of a 2000 psi expander cycle hydrogen fuel pump. The limited vehicle flight envelope may allow fixed geometry within the ram/scram flowpath, but variable geometry approaches are at reasonable levels (TRL 4-5) if needed. A hydrogen fuel-cooled flight-weight engine must be tested to verify engineering prediction of system durability. These experiments will provide a test bed for instrumentation to support future integrated vehicle health management. This development testing should be possible at small scale in an existing wind tunnel. Based on lessons learned in these systems tests, methods of testing critical flight-weight components at large or full scale using existing facilities must be developed. This will likely be direct-connect tests of the integrated isolator, combustor and nozzle, because the inlet shock structure is not critical to thermal loads and combustor performance at these lower Mach numbers. By limiting the maximum Mach number, this

approach may be possible with existing facilities, whereas it will not be possible for Mach 10-15 concepts. By limiting the Mach number to 7, existing ground test facilities may be used to bring durable scramjet engine component technology toward TRL 6. Life cycle can be demonstrated at modest scale in combustion-heated facilities (like the 8ft. HTT), which allow sufficient test time for the structure to reach near equilibrium Mach 7 temperature. Flight mission-length duration tests can be performed at smaller scale. If the flight engine is broken into small enough segments it may be possible to actually do these full-mission simulations in wind tunnel tests.

Two additional propulsion technical challenges must also be addressed. Integration of the turbojet and scramjet into a TBCC engine system (WBS 2.06) is a significant technical challenge (TRL 3-4). Integrated propulsion-airframe design/performance evaluation and thermal management (WBS 1.03) are also at a low TRL. This integration should be verified by tests in wind tunnels—a "relevant environment." Wind tunnel tests of turbojet engines are acceptable system demonstration for TRL 6. The Mach 7 flight of the X-43 demonstrated that wind tunnels are a relevant environment for scramjet demonstration to TRL 6. Therefore TBCC engine tests in wind tunnels meet the TRL 6 (relevant environment) requirement. However, continual variation of flight Mach number from sea-level-static to Mach 7 can only be performed in flight. Also, flight forces closer attention to details often overlooked by "physics based" analysis and wind tunnel tests. Low cost methods of testing and/or demonstrating these technologies may be possible. The simplest may be to fly the integrated system on a rocket booster, like the Russian Central Institute of Aviation Motors scramjet flying laboratory. However, a recovery system will be needed due to engine cost.

Integrated TBCC powered hypersonic vehicle TRL level of 6 cannot truly be achieved without a near-full scale flight test vehicle. However, completion of the above technology development provides a strong case to move to a large-scale research or prototype vehicle. Without first completing the above technology development and ground tests, a large scale research or prototype vehicle program may be doable, but it will be high risk.

Flight-testing is a natural evolution of any new aeronautical technology. Flight drives integration of all technologies required to complete a system which are generally developed separately before going to flight. Flight identifies challenges not generally known beforehand (unknown-unknowns). Flight generates customer, political and public interest. When to introduce flight-testing into a technology development program is an issue for thoughtful discussion. If funding is not highly constrained, flight-testing can move technology at a system level forward at a faster rate than possible without flight testing. If funding is constrained (as usual), careful consideration must be given before committing to flight research, or calling a technology development program a flight test program too early in its development. Whatever budget unfolds, flight must be a part of hypersonic air-breathing technology development. The challenges and successes associated with flight-testing will continue to attract bright students into the sciences and engineering. Flight-testing will be required for a few of the technology needs discussed.

7.0 SUMMARY AND CONCLUSIONS

Technology advances within the USA and around the world prove that efficient hypersonic flight is possible. The greatest benefit to mankind will be in space access applications. Development of safe, affordable, reliable, and reusable launch vehicles holds great promise as the key to unlocking the vast potential of space for business exploitation. Only when access to space is assured with a system that provides routine operation with orders-of-magnitude increased safety and at affordable cost will businesses be willing to take the risks and make the investments necessary to realize this great potential. Other applications - to military missions - are inevitable, and may be required to complete the transition from research to the commercial sector, and to convince the remaining sceptics. Exciting challenges remain, both technical and political.

8.0 REFERENCES

[1] H. Julian Allen, "Hypersonic Flight and the Re-entry Problem," The Twenty-First Wright Brothers Lecture. Journal of the Aerospace Sciences, Vol. 25, No. 4, April 1958.

[2] Riggins, D.W., McClinton, C.R., and Vitt, P.H., "Thrust Losses in Hypersonic Engines, AIAA Journal of Propulsion and Power," Vol. 13, No. 2, pp. 281-295, 1997.

[3] Escher, W.J.D, et.al., "A Study of Composite Propulsion Systems for Advanced Launch Vehicle Applications". The Marquardt Company Report 25, 194. Final Report, NASA Contract NAS7-337, 7 Volumes, Sept. 1966.

[4] Daines, R. and Segal, C., "Combined Rocket and Airbreathing Propulsion Systems for Space-Launch Applications," J. of Prop. And Power, vol. 14, no. 5, Sept/Oct 1998.

[5] Bogar, T.J., Eiswirth, E.A., Couch, L.M., Hunt, J.L., and McClinton, C.R., "Conceptual Design of a Mach 10, Global Reach Reconnaissance Aircraft," AIAA 96-2894, Jul. 1996.

[6] The Honorable Dr. Ron Sega, "Congressional Report on the National Aerospace Initiative," September 2003. http://www.dod.mil/ddre/nai

[7] Bilardo, V.J., Hunt, J.L., Lovell, N.T., Maggio, G., Wilhite, A.W., and McKinney, L.E., "The Benefits of Hypersonic Airbreathing Launch Systems for Access to Space," AIAA 2003-5265. July 2003, Huntsville, Al.

[8] Tandy, David, "Architecture C Limited Life Cycle Analysis. SAIC Presentation to NGLT," February 12, 2004.

[9] Scramjet Propulsion, AIAA Progress in Astronautics and Astronautics, Vol. 189, 2000. Chapter 6, Scramjet Performance Anderson, G.Y., McClinton, C.R., and Weidner, J.P.

[10] Henry, John R., and Anderson, Griffin Y., "Design Considerations for the Airframe-Integrated Scramjet," Presented at the 1st International Symposium on Airbreathing Engines, Marseille, France, June 1972 (also NASA TM X-2895, 1973).

[11] Andrews, Earl H., and Mackley, Ernest A., "Review of NASA's Hypersonic Research Engine Project," AIAA Paper 93-2323, June 1993.

[12] Pinckney, S. Z., "Rectangular Capture Area to Circular Combustor Scramjet Engine," NASA TM 78657, March 1978.

[13] Jacobs, P.A. and Craddock, C.S. "Simulation and Optimization of Heated, Inviscid Flows in Scramjet Ducts," J. of Propulsion and Power, vol. 15, No. 1, Jan.-Feb. 1999.

[14] McClinton, C.R., Hunt, J.L., Ricketts, R.H., Reukauf, P., and Peddie, C.L., "Airbreathing Hypersonic Technology Vision Vehicles and Development Dreams," AIAA Paper No. 99-4978, November 1999.

[15] Hicks, C.R., "Fundamental Concepts in the Design of Experiments", John Wiley and Son, New York, 1982.

[16] Montgomery, D.C., "Design and Analysis of Experiments", John Wiley and Son, New York, 1991.

[17] Box, G.E.P, and Draper, N.R., "Empirical Model-Building and Response Surfaces," John Wiley and Son, New York, 1987.

[18] McClinton, C.R., Ferlemann, S.M., Rock, K.E., Ferlemann, P.G., "The Role of Formal Experiment Design in Hypersonic Flight System Technology Development.," AIAA 2002-0543. Jan. 2002.

[19] Riggins, D. W., and McClinton, C. R., "A Computational Investigation of Mixing and Reacting Flows in Supersonic Combustors," AIAA 92-0626, Jan. 1992.

[20] Guy, R.W., et.al., "The NASA Langley Scramjet Test Complex," AIAA 96-3243. 32nd AIAA/ASME/SAE/ASEE Joint Propulsion Conference. Lake Buena Vista, FL, July 1-3, 1996.

[21] Andrews, E.H., "Scramjet Development and Testing in the United State," AIAA 2001-1927. April 24-27, 2001.

[22] Voland, R.T, et.al., "Hyper-X Engine Design and Ground Test Program," AIAA 98-1532.

[23] Roudakov, A.S., Y. Schickhman, V. Semenov, Ph. Novelli, and O. Fourt, "Flight Testing an Axisymmetric Scramjet: Russian Recent Advances, *in proceedings of 44th Congress of the International Astronautical Federation*, Oct. 16–22, 1993, Graz, Austria.

[24] Bittner, R. D., Private Communications, Nyma, Hampton Virginia.

[25] Rogers, R. C., Weidner, E. H., and Bittner, R. D., "Quantification of Scramjet Mixing in Hypervelocity Flow of a Pulse Facility," AIAA Paper 94-2518, June 1994.

[26] "NASP Phase 2D Final Scientific and Technical Report," A011 (DI-MISC-08711/T) F33657-91-L-2012, Dec., 94.

[27] Hunt, J.L., Ricketts, R.H. and McClinton, C.R., "Reference Technology Sets and Readiness Levels for Hypersonic Airbreathing Vehicles," 200 JANNAF CS, APS, PSHS and MSS Joint Meeting. Monterey, CA, Nov.13-17, 2000.

[28] Brown, R.L., "Assessing Technology Readiness Using a Value Stream Process. Presented at NET Workshop on Processes for Assessing Technology Maturation and Determining Requirements for Successful Infusion into Programs," Marshall Space Flight Center, Sep. 16-18, 2003.

[29] Committee on National Aerospace Initiative, Air Force Science and Technology Board, Division on Engineering and Physical Sciences, "Evaluation of the National Aerospace Initiative. National Research Council of the National Academies," The National Academies Press, Washington, D.C., April 2004.

[30] Bowcutt, K.G, and Hatakeyama, S.J., "Challenges, Enabling Technologies and Technology Maturity for Responsive Space," AIAA 2nd Responsive Space Conference. AIAA 2004-6005.

[31] McClinton, C.R., Rausch, V.L., Shaw, R.J., Metha, U., and Naftel, C., "Hyper-X, Foundation for Future Hypersonic Launch Vehicles," IAC-04-V.8.08. Sept, 2004.

[32] "Decadal Survey of Civil Aeronautics – Foundation for the Future," National Research Council, The National Academes Press, Washington, D.C. www.nap.edu.

[33] Curran, E.T., Scramjet Engines: The first Forty Years. J. Propulsion and Power, Vol. 17, No. 6, Nov-Dec 2001.

[34] Why and Whither: Hypersonics Research in the US Air Force. United States Air Force Scientific Advisory Board. SAB-TR-00-03, Dec. 2000.

[35] Gibson, C.S., Vess, R.J., and Pegg, R., Low Speed Flight Testing of a X-43A Hypersonic Lifting Body Configuration. AIAA 2003-7086, Dec. 2003.

[36] Pittman, J.L., NASA Hypersonics Project Overview. Presented at 14th AIAA/AHI International Space Planes and Hypersonic Systems and Technologies Conference. Nov. 2006. http://www.aiaa.org/pdf/conferences/hypersonics06nasa.pdf

[37] Jackson, K.Y., Scramjet Engine Gears up for Flight Tests. *News at AFRL*. http:/www.afrl.af.mil/news/mar06/features/flight_tests.pdf

[38] Rausch, V.L., "NASA Scramjet Flights to Breath New Life into Hypersonics," Aerospace America, vol 35, No 7, pp 40-46, July 1997.

[39] Engelund, W.C., Hyper-X Aerodynamics, "The X-43A Airframe-Integrated Scramjet Propulsion Flight Test Experiments," Journal of Spacecraft and Rockets, Vol 38, No. 6, Nov-Dec 2001. pg. 801-802

[40] Engelund, W.C., et.al., "Aerodynamic Database Development for the Hyper-X Airframe-Integrated Scramjet Propulsion Experiments," Journal of Spacecraft and Rockets, Vol 38, No. 6, Nov-Dec 2001. pg. 803-810.

[41] Reubush, D.E., "Hyper-X Stage Separation-Background and Status," AIAA Paper 99-4818, Nov. 1999.

[42] Woods, W.C., Holland, S.D., and DiFulvio, M., "Hyper-X Stage Separation Wind Tunnel Test Program," Journal of Spacecraft and Rockets, Vol 38, No. 6, Nov-Dec 2001. pg. 811-819.

[43] Buning, P.G., Wong, T., Dilley, A.D., and Pao, J.L., "Computational Fluid Dynamics Predictions of Hyper-X Stage Separation Aerodynamics," Journal of Spacecraft and Rockets, Vol 38, No. 6, Nov-Dec 2001. pg. 820-827.

[44] Holland, S.D, Woods, W.C., and Engelund, W.C., "Hyper-X Research Vehicle Experimental Aerodynamics Test Program Overview," Journal of Spacecraft and Rockets, Vol 38, No. 6, Nov-Dec 2001. pg. 828-835.

[45] Berry, S.A., Auslender, A.H., Dilley, A.D., and Calleja, J.F., "Hypersonic Boundary Layer Trip Development for Hyper-X," Journal of Spacecraft and Rockets, Vol 38, No. 6, Nov-Dec 2001.

[46] Huebner, L.D., et.al. "Hyper-X Flight Engine Ground Testing for Flight Risk Reduction," Journal of Spacecraft and Rockets, Vol 38, No. 6, Nov-Dec 2001. pp 844-852. pg. 853-864.

[47] Cockrell, C.E., et.al.., "Integrated Aeropropulsive Computational Fluid Dynamics Methodology for the Hyper-X Flight Experiment," Journal of Spacecraft and Rockets, Vol 38, No. 6, Nov-Dec 2001. pp 844-852. pg. 836-843.

[48] Keel, L.C., "X-43 Research Vehicle Design and Manufacture," AIAA 2005-3334.

[49] Harsha, P.T., Keel, L.C., Castrogiovanni, A., and Sherrill, R.T., "X-43 Vehicle Design and Manufacture," 13th International Space Planes and Hypersonic Systems and Technology Conference, Capua, Italy. May 2005.)

[50] Redifer, M.E., Lin, Y., Kelly, J., Hodge, M., and Barklow, C., "The Hyper-X Flight System Validation Program," Hyper-X Program Office Report, HX-849. 2003.

[51] Joyce, P.J., and Pomroy, J.B., "Launch Vehicle Design Challenges for Hypersonic Flight Testing (Mach 7 and 10)," 28th JANNAF Air-breathing Propulsion Subcommittee Meeting. Charleston, SC. June 13-17, 2005

[52] Corpening, G., Marshall, L., Sherrill, R., and Nguyen, L., "A Chief Engineer's View of NASA's X-43 Scramjet Flight Test," AIAA 2005-3332, Capua, Italy. May 2005.

[53] Marshall, L., Bahm, C., Corpening, G., and Sherrill, R., "X-43 Flight 3 Preparation and Results," AIAA 2005-3336, Capua, Italy. May 2005.

[54] Bahm, C., Stovers, B., Baumann, E., Beck, R., Bose, D., "X-43 Guidance, Navigation and Control Challenges," AIAA-2005-3275, Capua, Italy. May 2005.)

[55] Morrelli, E.A., "Aerodynamic Parameter Estimation for the X-43A from Flight Data," AIAA 2005-5921

[56] Karlgaard, C.D.; Hyper-X Post–Flight Trajectory Reconstruction. AIAA 2004-4829, Aug. 2004

[57] Blocker, W, et.al.., "X-43 Stage Separation Analysis – A Flight Data Evaluation," AIAA 2005-3335. May 2005.

[58] Engelund, W.C., "Aerodynamics, Results from the Mach 7 & Mach 10 Scramjet Flight Tests," AIAA 2005-3405,

[59] Storch, A.R., Ferlemann, S.M, Bittner, R.D., "Hyper-X, Mach 7 Scramjet Preflight Predictions versus Flight Results," 28th JANNAF Air-breathing Propulsion Subcommittee Meeting. Charleston, SC. June 13-17, 2005.

[60] Pinckney, S.Z., Ferlemann, S.M., Mills, J.C., and Bass, L.S., "Program Manual for SRGULL," HX-829.1, Dec. 04.

[61] Lockwood, M.K., et.al., "Design and Analysis of a Two-Stage-to Orbit Airbreathing Hypersonic Vehicle Concept," AIAA 96-2890. July 1-3, 1996.

[62] Ferlemann, P.G., "Improvements to the SHIP Computer Code and Predictions of Vorticity Enhanced Turbulent Supersonic Mixing," M.S. Thesis. School of Engineering and Applied Sciences. GWU, Washington, D.C.

[63] Ferlemann, S.M., Voland, R.T., Cabell, K, Whitte, D., and Ruf, E., "Hyper-X Mach 7 Scramjet Pretest Predictions and Ground to Flight Comparison," AIAA 2005-3322Capua, Italy. May 2005.

[64] Ferlemann, P.G., "Hyper-X Mach 10 Scramjet Preflight Predictions vs. Flight Data," AIAA 2005-3352. Presented at 13th International Space Planes and Hypersonic Systems and Technology Conference, Capua, Italy. May 2005.

[65] Rogers, R.C., "Scramjet Engine Flowpath Development for the Hyper-X Mach 10 Flight Test," ISABE 2005-1025.

[66] Berry, S.A., Boundary Layer Transition on the X-43A Flight 2. 28th JANNAF ABPS Meeting, June 2005.

[67] McClinton, C.R., X-43 – "Scramjet Power Breaks the Hypersonic Barrier," The AIAA Dryden Lectureship in Research for 2006. AIAA 2006-0001. Jan. 2006.

[68] Roudakov, A.S., et.al, "Recent Flight Tests of the Joint CIAM/NASA Mach 6.5 Scramjet Flight Program," NASA TM-1998-206548, April, 1998.

[69] Voland, R.T., et.al., "CIAM/NASA Mach 6.5 Scramjet Flight Test," AIAA 1999-4848, Nov. 1999.

[70] McNelis, N. and Bartolotta, P., "Revolutionary Turbine Accelerator (RTA) Demonstrator," AIAA 2005-3250. AIAA 13th HyTASP Conference. 2005.